Water adsorption on hydroxylated α-quartz (0001) surfaces: From monomer to flat bilayer

Jianjun Yang and E. G. Wang*
Beijing National Laboratory for Condensed Matter Physics and Institute of Physics, Chinese Academy of Sciences, Box 603, Beijing 100080, China

(Received 23 June 2005; revised manuscript received 6 September 2005; published 5 January 2006)

Water adsorption on the hydroxylated α-quartz (0001) surface at various coverages was studied using *ab initio* total energy calculations and molecular dynamics simulations within density functional theory. The relaxed geometry of the clean surface is characterized with zigzag hydrogen-bond (H-bond) chains of vicinal surface hydroxyls, with strong and weak H-bond interactions appearing alternatively along them. Upon water adsorption, the weak H-bonds on the surface are broken and the corresponding hydroxyls reform H-bonds with the adsorbed molecules, e.g., two H bonds for an isolated water monomer/dimer. Increasing the water adsorption to one monolayer, we find an ordered hexagonal water layer on the oxide surface with a flat bilayer structure, compared with the basal plane of ice Ih. The H-down bilayer configuration is more favored than the H-up bilayer from both the energetic and dynamic points of view. In addition, two kinds of H-bonds with different strengths are identified in the bilayer from the vibrational spectra of the OH stretch modes. The origin of these two kinds of H-bonds is different in nature from those reported in the recent studies of a tessellation ice on the hydroxylated β-cristobalite (100) surface and a bilayer structure on metal Pt (111) surface.

DOI: 10.1103/PhysRevB.73.035406 PACS number(s): 68.43.Bc, 82.30.Rs, 68.35.−p

I. INTRODUCTION

The interaction between water and solid surfaces is of fundamental interest in materials science and biological systems.[1,2] Much work has been done to investigate the adsorption of water on metal[3,4] and oxide surfaces.[5–8] It is well reviewed by Ref. 1 that the adsorption of water can be either molecular or partially dissociative, depending on the water coverage. Depending on the system, adsorbed water on surfaces has been detected as monomers, small clusters, one-dimensional (1D) chains, two-dimensional (2D) ordered overlayers, and a variety of ice structures.[2]

Among the oxides, silica (SiO_2) is the most abundant natural mineral on Earth. Water-silica interactions play an important role in many natural processes and advanced technological applications, such as weathering, corrosion, dissolution, and catalysis.[9,10] Water is inevitably present in nature and in so many technological applications. Hence, the interaction of water with silica has been the subjects of a wide range of investigations both experimentally[11–17] and computationally.[18–24] The experiments have provided a large volume of data. It is believed that a freshly formed silica surface is often hydroxylated rapidly through the reaction with atmospheric moisture.[9] For example, exposure of fractured silica surface to water vapors with partial pressure higher than 1.33×10^{-7} Pa results in the hydrolysis of surface sites with the formation of silanol groups (Si-OH), which is completed with 1 h.[25] Similarly, the surface of α-Al_2O_3 (0001) has also been exemplified with the termination of hydroxyl groups (-OH) under a humid environmental condition.[26] Silanol groups have been detected on silica surfaces by experiments.[11–13] The precursor to the fully hydroxylated surface is a bare silica surface, and many efforts have been dedicated on the study how water dissociates on the crystalline quartz and amorphous silica surface and how these silanols are formed.[21–24] The molecular and dissociative adsorption of water has been studied (using the shell model) on bare quartz surfaces,[27] and the results indicated that dissociative adsorption is thermodynamically favorable. As is known the reactive chemical and physical properties of the hydroxyl groups on the silica surface are, by and large, responsible for the widespread utility in the technological applications. The surface silanol groups have a high polarity that is very sensitive to the adsorption of small gaseous molecules such as H_2O, NH_3, etc., while the adsorbed molecules will definitely have an effect on its surface reactivity in turn. The interaction of water molecules with the silica surface hydroxyls has ever been studies widely within various cluster models.[28] However, to our knowledge, very limited theoretical works have been devoted to the study of water adsorption on the hydroxylated silica surface within *ab initio* calculations so far,[27] except for our previous studies on the hydroxylated surfaces of β-cristobalite,[29,30] another phase of crystalline silica.

To gain more insight on the adsorption of water on hydroxylated silica surfaces, the use of the α-quartz (0001) surface as a substrate reveals particularly interesting since it sustains typical silanols found on most silica surfaces. In addition, α-quartz is one of the most abundant natural minerals on earth, and it is the most stable crystalline silica (SiO_2) phase over a broad range of temperatures and pressures, including ambient conditions. It is often used in technological applications and scientific research.[15–18,27,31–34] Its clean (0001) face with hexagonal symmetry is found to be the most stable surface.[27,33] Recently, various possible surface structures of α-quartz (0001) were proposed by Rignanses *et al.*,[31] and then the hydration mechanisms were investigated on some typical structures using first-principle molecular calculations.[32] Also, within DFT calculations the water adsorption at two (0001) surfaces was studied by de Lueew *et al.* very recently.[18] As for the case of fully hydroxylated α-quartz surfaces, the (0001) face was also re-

TABLE I. Calculated and experimental (Ref. 40) lattice constants a and c (in Å), Si-O bond lengths (in Å), bond angles ∠SiOSi and ∠OSiO (in degree) for α-quartz crystal with hexagonal symmetry.

	a	c	Si-O	∠SiOSi	∠OSiO
Theor.	4.910	5.404	1.610	143.30	108.57, 108.72, 108.97, 110.66
Expt.	4.913	5.404	1.600	143.73	108.81, 108.93, 109.24, 110.52

ported to be the most stable one within density functional theory (DFT) calculations,[33] where the H bonds between vicinal silanol groups play a key role in its stability.

In this work, our aim is to investigate the atomic structures and energetics of adsorbed water on the hydroxylated α-quartz (0001) surface at various coverages, including species such as monomer, dimer, and monolayer, using first-principles calculations. The optimized structure of the hydroxylated α-quartz (0001) surface is determined first. Its salient characteristic is the zigzag hydrogen-bond (H-bond or HB) chains of the vicinal hydroxyls formed with appearances of strong and weak HBs alternatively along them. When water is added, those weak surface HBs are broken and the corresponding hydroxyls reform H bonds with H_2O molecules simultaneously. Consequently, the water monomer and dimer usually adsorb on the weak surface HB sites, forming H bonds with the surface hydroxyls. Upon increasing the adsorbed molecules to one monolayer coverage (i.e., one H_2O per surface hydroxyl group, in accord with the definition in Ref. 30), we have determined an ordered 2D water layer structure on the surface. It is identified as a flat hexagonal bilayer structure, very similar to the basal plane in bulk ice Ih.[1] In fact, the similar ordered hexagonal 2D bilayer structure was first proposed experimentally by Doering and Madey in the early 1980s.[35] In contrast with the energy-degenerated nature of H-up and H-down bilayers ever found on metal surfaces,[36] our calculations show the H-down configuration is energetically much more favored on hydroxylated α-quartz (0001) than the H-up one from both the energetic and dynamic points of view. Because of the strong H-bonding nature between the surface hydroxyls with both types of adsorbed molecules, the H-down bilayer found here is flatter than it is on metals. Besides, a further vibrational analysis indicates there are two kinds of HBs with different strengths in the bilayer structure and indicating no free OH bond existing in the water bilayer. The partition between the strong and weak HBs originates in a way that differs from those reported in the 2D water layers on metal Pt (111)[36] and hydroxylated β-cristobalite (100).[29]

The rest of the paper is organized as follows. In Sec. II, the computational methods are described. The main results and discussion are presented in Sec. III. And a summary is given in Sec. IV.

II. COMPUTATIONAL DETAILS

Total energies and MD simulations were calculated within the framework of DFT using the plane-wave-based Vienna *ab initio* Simulation Package (VASP).[37] The Perdew and Wang (PW91) version of generalized gradient approximation[38] (GGA) was used as the exchange-correlation function. GGA extension is crucial for the accurate treatment of the hydrogen bonds and water structures, and the PW91 form has been test extensively for a variety of intermolecular interactions including H bonding.[30,36] The energy cutoff was fixed at 350 eV for statics and 300 eV for MD calculations. Electron-ion interactions were described using ultrasoft pseudopotentials (UPP).[39] The structural relaxation was performed with a conjugate gradient algorithm. The optimization was terminated when the forces on all relaxed atoms were smaller than 0.03 eV/Å. In MD simulations, the water molecules and the surface atoms were allowed to move according to the forces calculated from the converged electronic structure. The vibrational spectrum was obtained by performing Fourier transformation of velocity autocorrelation function, which was recorded in our MD simulations. To obtain the vibrational spectra, a MD simulation run with a time step of 0.5 fs has been performed for typically 2 ps at 80 K after equilibrating the system for 1 ps. A longer simulation time of 4 ps and/or a shorter time step of 0.25 fs did not change the peak positions and the shape of the vibrational spectra.

Quartz has a hexagonal structure with space group $P3_121$.[40] Table I summarizes the optimized bulk α-quartz structure, which shows the good agreement between our *ab initio* calculations and experiments. To model (0001) surfaces, we used a tetragonal supercell with a slab of SiO_2 and a vacuum layer of about 10 Å. We checked convergence by running a series test calculations with different SiO_2 slab thickness. A slab with three O-Si-O layers was used, which has an energy convergence within 0.023 eV. The initial configuration of the completely hydroxylated surface was obtained by saturating those terminal O atoms on both the top and bottom surfaces with hydrogen atoms. The top surface was used to represent the completely hydroxylated surface, while the two atomic layers on the bottom surface were fixed during all calculations to model the bulk substrate. The resulting supercells were subjected to periodic boundary conditions. Two different tetragonal supercells $9.820\times8.504\times20$ Å^3 for cluster-adsorbed surface and $4.910\times8.504\times20$ Å^3 for bilayer-adsorbed surface, were used. The Brillouin-zone integration was performed on special grids as proposed by Monkhorst and Pack.[41] The k-point mesh was sampled using a single Gamma point and $2\times2\times1$ for the above two supercells, respectively, which give the total energy convergence within 0.01 eV.

Finding a transition state requires the determination of minimum energy pathway (MEP) for the reaction under investigation, with the transition state being the saddle point along the MEP. The nudged elastic band (NEB) method,[42] available in VASP, was applied to scan potential energy sur-

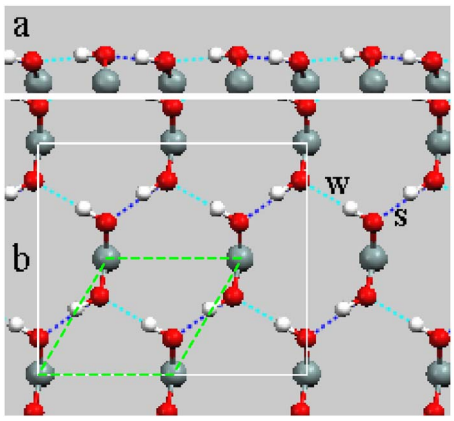

FIG. 1. (Color online) Optimized geometry for the clean hydroxylated α-quartz (0001) surface: side view (a) and top view (b). For clarity, only the surface atoms are depicted here: large gray spheres for silicon, middle-size black spheres for oxygen, and small white spheres for hydrogen, respectively. The strong (SHB) and weak (WHB) surface H bonds are depicted with dark and light gray dotted lines and marked as S and W, respectively. The gray dashed lines show the hexagonal surface unit cell, while the white lines depict the tetragonal surface cell used in the present work.

faces searching for reasonable MEPs. An initial guess with four "images" between initial and final states was continuously refined around the prospective saddle point until the distances between the images in phase space are small enough to apply the climbing image C-NEB.[43]

The adsorption energy E_{ads} per water molecule is calculated by $E_{ads}=-(E_{total}-E_{surf}-nE_{H_2O})/n$, where E_{total} is the energy of the adsorption system, E_{surf} is the energy for the optimized clean hydroxylated surface system, E_{H_2O} is the energy for an isolated water molecule in gas phase, and n is the number of adsorbed water molecules.

III. RESULTS AND DISCUSSION

A. Geometry of the clean surface

The structure of the fully hydroxylated α-quartz (0001) surface is relaxed before water adsorption, within the tetragonal surface cell (9.820×8.504 Å^2). The optimized geometry is presented in Fig. 1. The surface is completely covered with geminal silanol groups [Si-$(OH)_2$]. All its hydroxyl groups lie almost in the same plane parallel to the surface, facilitating the formation of surface H bonds between two nearest vicinal hydroxyls. As in our previous work[30] we assume the hydrogen bond is formed when the OO distance is less than 3.30 Å and the O-H-O angle is greater than 140° (the OO distance of the H bond in ice Ih is ~2.76 Å), then those surface HBs can be divided into two kinds with different strengths. The stronger one (with OO distance of 2.72 Å and OH-O angle of 168°) and the weaker one (with OO distance of 3.09 Å and OH-O angle of 171°) are denoted as SHB and WHB (i.e., the H…O lengths of 1.74 and 2.11 Å), respectively (see Fig. 1). Strikingly, zigzag chains of H-bonded surface hydroxyls are formed with SHB and WHB appearing alternatively. Apparently, this surface geometry

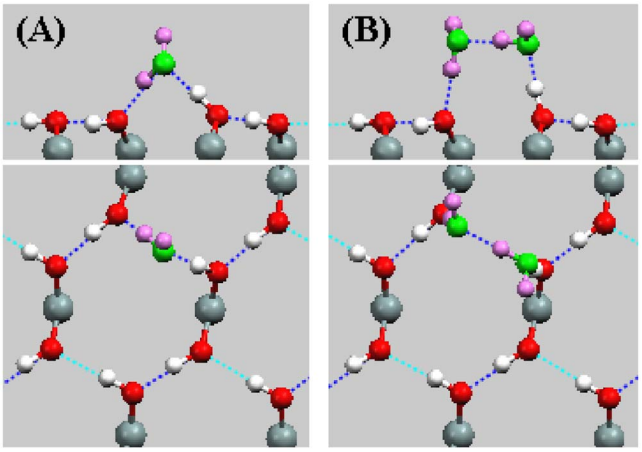

FIG. 2. (Color online) Optimized geometries for adsorbed monomers (A) and dimers (B) depicted both from the side view and the top view. The oxygen (O_w) and hydrogen (H_w) in the adsorbed H_2O are colored differently from those on surfaces: middle gray (green) for O_w and small light gray (violet) for H_w.

differs to some extent from that reported in a recent work on the same surface by Murashov,[33] where only one kind of HB was found and half of the hydroxyls were not included in surface H-bonding interactions. The difference most likely comes from the different accuracy requested for convergence of the structural optimizations in both works. The similar H-bond chains have ever been found on the relaxed hydroxylated β-cristobalite (100) face.[29]

B. Isolated water monomer and dimer adsorption

An isolated water monomer adsorption on the hydroxylated α-quartz (0001) surface was studied. Several different symmetric configurations for water adsorption have been studied. We find the most preferred position for the adsorbed molecule is to sit above the WHB site, as shown in Fig. 2(a). Due to the high polarity of both H_2O molecules and surface hydroxyls, there is a competition of the H-bonding interaction between hydroxyl-water and hydroxyl-hydroxyl. The predominance of the hydroxyl-water interaction is obvious, resulting in the original weak H bond of hydroxyl-hydroxyl broken, and the corresponding hydroxyl group being lifted up from the surface plane by reforming an H bond with the adsorbed water molecule. Therefore, the molecule is stabilized on the surface through the formation of two H bonds with the hydroxyl groups—one as a proton-acceptor and the other as a proton donor [see Fig. 2(a)]. The OO distances of the two HBs between the molecule and surface are 2.57 and 2.70 Å (i.e., the H…O lengths of 1.56 and 1.73 Å, respectively)—even shorter than that for an SHB interaction (2.72 Å).

The adsorption energy of a water monomer on the hydroxylated α-quartz (0001) surface is 543 meV/H_2O—comparable with that on the hydroxylated β-cristobalite (100) surface (528 meV/H_2O).[30] Fubini *et al.*[44] used microcalorimetric measurements to find adsorption energies of water on powdered quartz, which can be expected to contain a wide range of surfaces. They found at

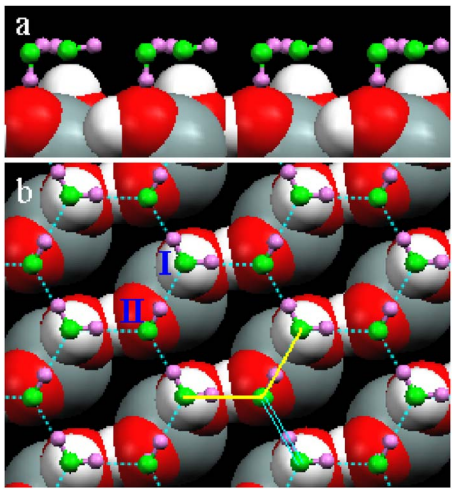

FIG. 3. (Color online) Optimized H-down bilayer geometry on the hydroxylated α-quartz (0001) surface: side view (a) and top view (b). For clarity of the adsorbed bilayer structure, the substrate atoms are depicted as space-filled spheres here. Dotted lines denote the H-bond interactions between adsorbed molecules. The single-line (yellow) and double-line (light blue) depict the strong and weak HBs in the bilayer structure, respectively.

higher partial water pressures the adsorption energy approached a constant value of approximately 518 meV/H_2O (50 kJ mol^{-1}) and predicted to corresponding to the physisorbed water species, which is much close to our result given above. In fact, when the water molecule is put at the SHB site initially, the strong H bond can be broken too, but that configuration is less stable by 115.3 meV/H_2O because of the comparable H-bonding interactions between the hydroxyl-water and hydroxyl-hydroxyl.

Water dimer adsorption is found to be most likely on the WHB site also, as shown in Fig. 2(b). Its optimized geometry looks quite similar to its gas-phase counterpart.[45] The two molecules in the dimer are adsorbed nearly atop the two hydroxyls at the WHB site, respectively, through H bonding. The adsorption energy is reduced to 475 meV/H_2O, due to the decreased number of the HBs between the water and the surface. The much-reduced OO distance of 2.63 Å in the adsorbed dimer (2.90 Å for free dimer) clearly indicates that the adsorption enhances H bonding inside the dimer.

C. Bilayer adsorbed structure

Upon increasing the water adsorption to one monolayer coverage, a flat bilayer structure can be distinctly recognized from the extended structure, as shown in Fig. 3, with water molecules forming a puckered hexagonal network, similar to that in bulk ice Ih.[1] In this icelike bilayer structure, there are two types of water molecules according to their different ways of interacting with the surface. Type I (denoted in Fig. 3) sits nearly parallel to the surface by accepting an H bond from one lifted surface hydroxyl group, and type II points one of its OH bonds down to the oxygen of the other adjacent surface hydroxyl. Obviously, each H_2O molecule is H bonded with its three neighbors and a surface hydroxyl. The bilayer in Fig. 3 is usually denoted as H-down structure, according to the downward OH bond configuration in type II.

TABLE II. Calculated O-O distances (in Å) of water-water (O_w-O_w), water-surface (O_w-O_s), and hydroxyl-hydroxyl (O_s-O_s) contacts for the ice bilayers on the hydroxylated α-quartz (0001) surface. The O-O distance in the ordinary ice Ih is 2.76 Å.

	O_w-O_w	O_s-O_w	O_s-O_s
Clean surface			2.72, 2.73, 3.09
H-down bilayer	2.77, 2.87	2.67, 2.72	2.55, 2.63, 3.44
H-up bilayer	2.85, 2.87, 2.90	2.74, 3.24	2.54, 2.59, 3.50

In the H-down bilayer structure, we note that half the water molecules with type I lie in the upper plane, and each of them donates its two OH bonds to the neighboring type II molecules in the lower plane. This icelike bilayer structure has been found on many hexagonally close-packed transition metal surfaces,[36] but usually the type I plane is lower than the type II plane. The reason we call it a flat bilayer is that the vertical distance between the two oxygen atoms in the two planes is as small as 0.1 Å, which is at most one-third of that on metal Pt (111) (Ref. 8, and references therein) and about one-tenth of that in bulk ice (0.97 Å).[1] This great compression, compared to bulk ice and those ice bilayers on most metals, is attributed to the strong H-bonding interactions (see Table II) between the surface and both the type I and II adsorbed molecules. In fact, a similar flat bilayer structure has also been reported in the case of D_2O on Ru (0001).[46]

The adsorption energy of this H-down bilayer is 650.5 meV/H_2O, which is higher than that of an isolated molecule (576.5 meV/H_2O). Most of the adsorption energy gain in the bilayer structure is due to the formation of lateral H-bonding interactions between molecules. Accordingly, the water-surface interaction is reduced with respect to the adsorption of a single water molecule.

For comparison with previously described bilayers on metal surfaces,[36] we also determine the H-up bilayer geometry (one OH bond of type II molecule directed upward from the surface). In our optimized H-up structure, we find the two layers are reversed completely; that is, the lower layer is built up with type I water molecules instead of type II. In addition, the vertical OO distance of the bilayer in this case increases to 0.47 Å. All these details indicate a different nature of surface-water (type II) interaction. Type II molecules are not H-bonded with the surface anymore and one of its OH bonds extends upwards freely, lifting up the type II layer and increasing the vertical spacing.

We find that the H-up structure is less stable than the H-down one due to the large reduced adsorption energy of ΔE_{ads}=188.2 meV/H_2O. This indicates that the H-up configuration is not energetically favored on the surface. However, it is still very interesting and necessary to study the energy barrier and the MEP, from the viewpoint of dynamics, when the H-up structure transforms into the H-down bilayer. The calculated MEP and the schematic transition state (saddle point) are shown in Fig. 4. The MEP involves mainly the rotation of the type II molecule inside its HOH plane, together with a little shifting vertically. The type II molecule

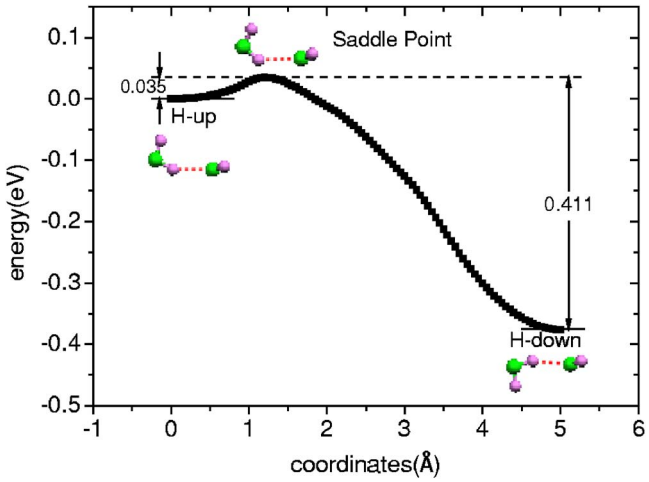

FIG. 4. (Color online) The minimum energy pathway (MEP) and the schematic transition state (saddle point) for a type II molecule from H-up to H-down bilayers on the hydroxylated α-quartz (0001) surface.

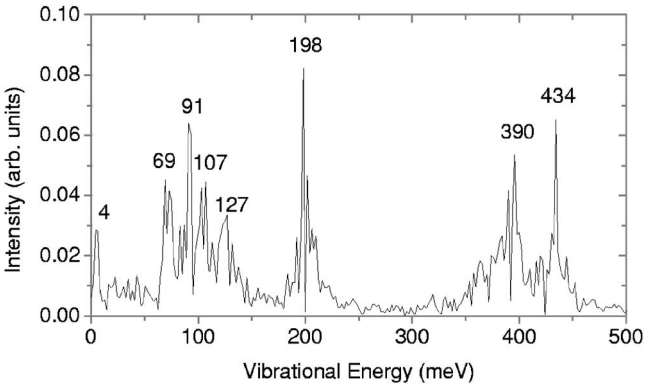

FIG. 5. The vibrational spectrum for the H-down bilayer at $T=80$ K.

rotates over about 56° in total along the MEP in the transitional process. The energy barrier for the H-up bilayer to flip to H-down is found to be 35 meV per type II molecule, which takes place at the molecule rotation of 9°. This barrier is so small—only half of that in a free dimer of 78 meV[47]—that it can be easily overcome during the transformation from a H-up bilayer to a H-down one. This process is almost irreversible, as the corresponding energy barrier is as high as 411 meV in the reversed process (see Fig. 4). Therefore, we conclude that the H-down bilayer is much more favored on the hydroxylated α-quartz (0001) surface than the H-up one, from both the energetic and dynamic points of view. This is clearly different from the cases on transition metal surfaces,[36] where both H-down and H-up configurations are degenerated in energy and thus are able to coexist.

Similar to those bilayers found on most close-packed transition metal surfaces[36] which are very dependent on the commensurate surface structures with a face of ordinary Ih (hexagonal) ice, the ice bilayer predicted here on the hydroxylated α-quartz (0001) surface arises mainly from the interesting structure of the basal plane. The α-quartz (0001) surface has a hexagonal lattice constant of 4.91 Å, which is comparable with the periodicity in bulk ice Ih (4.52 Å).[48] Therefore, the surface oxygen atoms of hydroxyls, two in each unit cell, form a pseudohexagonal structure very similar to the hexagonal ice structure (see Fig. 1 and the O_s-O_s distances in Table II). Consequently, each adsorbed water molecule interacts via hydrogen bonding with a surface OH group, epitaxially forming an ordered water layer with ice-like structure.

D. Vibrational characteristics

Vibrational spectra have proved to be quite useful for the identification of surface and interface structures experimentally, especially for the H-bonded water systems. To provide a database for vibrational recognition of the identified H-down bilayer structure on the hydroxylated α-quartz (0001) surface, we calculated the vibrational spectrum as shown in Fig. 5. We note there are three main regions: the lower frequency region (<130 meV) for the intermolecular translational and librational vibrations; the HOH bending mode at 198 meV; and the OH stretching modes at the higher frequency region (>300 meV). It is interesting to analyze the vibration modes in the OH stretching region, because they are very sensitive to the variation of the H-bonding environment. The stronger the H bond is, the more redshifted the stretch mode appears, compared to that of the free OH bond in gas phase water molecules. The calculated values of the free OH bond vibrations of a free water molecule are 462 meV (symmetry) and 478 meV (asymmetry), which are in good agreement with the experiments[49] of 454 and 466 meV, respectively.

In Fig. 5, we find all high frequencies modes redshifted, which indicate that no free OH bond is present in the bilayer structure. It is therefore speculated that the lack of OH groups pointing upwards should be also noticed in the future x-ray adsorption experiments. Together with the analysis of a certain OH bond vibration by tracking its trajectory, two distinct vibrational modes located at 390 and 434 meV are identified from two kinds of H bonds with different strengths in the H-down bilayer structure. They correspond to the two different O_w-O_w distances of 2.77 Å (stronger) and 2.87 Å (weaker) (i.e., the H…O length of 1.79 and 1.92–1.95 Å, respectively), in the bilayer structure, as indicated with the (yellow) single-line and (blue) double-line in Fig. 3. Apparently, the left (yellow) single-line and the (blue) double-line are symmetric in the bilayer itself. The reason that one is weak and the other is strong is attributed to the unique underlying substrate structure, for example, the two different surface HBs (strong and weak) and thus the different site distances. A further analysis shows that the H bonds provided by water to surface are a little stronger with shorter O_s-O_w distances, shown in Table II, and they are also partially incorporated with the vibration peak of 390 meV.

In a word, two kinds of HBs with different strengths can be identified in the H-down bilayer structure on the hydroxylated α-quartz (0001) surface, which is very relevant to the underlying substrate structure. The similar partition of two different H bonds was also reported in the bilayer on metal

Pt (111) (Ref. 36) and in the tessellation ice structure on hydroxylated β-cristobalite (100),[29] but they originate differently in nature. The origination on Pt (111) is from different numbers of HBs the water molecule donating in the bilayer structure; while on hydroxylated β-cristobalite (100) it is from different connections served inside or outside the four-membered water rings in the tessellation ice structure.

IV. SUMMARY

Using first-principles density functional theory calculations, we have investigated the geometries of the hydroxylated α-quartz (0001) surface with and without water adsorption. The optimized geometry of the clean hydroxylated α-quartz (0001) surface is characterized with zigzag chains composed of H-bonded vicinal surface hydroxyls, with the appearance of strong and weak HBs alternatively along them. When water is adsorbed on it, we find the original weak surface H bonds will be broken and new H bonds are formed between the corresponding hydroxyls and the adsorbed water molecules.

When the adsorbed water molecules are increased to one monolayer, a flat hexagonal H-down bilayer structure is distinctly identified, very similar to the basal plane in the normal ice Ih. Because of the strong H-bonding nature between the hydroxylated α-quartz (0001) surface and the two types of adsorbed molecules, the bilayer structure reported here is more flat than any similar structures on metal surfaces. Also in contrast with the energy-degenerated nature of H-up and H-down bilayers on metal surfaces, the H-down configuration reported here is more favored than the H-up one from both energetic and dynamic points of view. Consequently, the surface activity of the hydroxylated α-quartz (0001) surface under humid conditions would be suppressed with the H-down water bilayer present, where no free OH group is available on the surface any more. Besides, the division of two kinds of H-bonds in the H-down bilayer from the vibrational analysis is closely related with the underlying substrate structure for the hydroxylated α-quartz (0001), while it originates differently from that on metal Pt (111) surface and that in the tessellation ice structure on hydroxylated β-cristobalite (100). Furthermore, this bilayer structure on the hydroxylated α-quartz (0001) surface is also dependent on the commensurate lattice symmetry of the substrate compared with bulk ice Ih.

ACKNOWLEDGMENTS

We thank Professor Y. R. Shen for his stimulating discussion and Mike Dotson for his critical reading of this manuscript. This work has been supported by the NSF, MOST, and CAS of China.

*Email address: egwang@aphy.iphy.ac.cn

[1] P. A. Thiel and T. E. Madey, Surf. Sci. Rep. **7**, 211 (1987).
[2] M. A. Henderson, Surf. Sci. Rep. **46**, 1 (2002).
[3] T. Mitsui, M. Rose, E. Fomin, D. Ogletree, and M. Salmeron, Science **297**, 1850 (2002).
[4] P. Feibelman, Science **295**, 99 (2002).
[5] M. Odelius, Phys. Rev. Lett. **82**, 3919 (1999).
[6] L. Giordano, J. Goniakowski, and J. Suzanne, Phys. Rev. Lett. **81**, 1271 (1998).
[7] K. C. Hass, W. F. Schneider, A. Curioni, and W. Andreoni, Science **282**, 265 (1998).
[8] C. Zhang and P. J. D. Lindan, J. Chem. Phys. **118**, 4620 (2003).
[9] *The Chemistry of Silica*, edited by R. K. Iler (Wiley, New York, 1979).
[10] *The Surface Properties of Silica*, edited by A. P. Legrand (Wiley, New York, 1998).
[11] D. R. Kinney, I. S. Chuang, and G. E. Maciel, J. Am. Chem. Soc. **115**, 6786 (1993).
[12] I. S. Chuang and G. E. Maciel, J. Am. Chem. Soc. **118**, 401 (1996).
[13] Y. D. Kim, T. Wei, J. Stultz, and D. W. Goodman, Langmuir **19**, 1140 (2003).
[14] S. Engemann, H. Reichert, H. Dosch, J. Bilgram, V. Honkimaki, and A. Snigirev, Phys. Rev. Lett. **92**, 205701 (2004).
[15] V. Ostroverkhov, G. A. Waychunas, and Y. R. Shen, Chem. Phys. Lett. **386**, 144 (2004); Q. Du, E. Freysz, and Y. R. Shen, Phys. Rev. Lett. **72**, 238 (1994).
[16] V. Ostroverkhov, G. A. Waychunas, and Y. R. Shen, Phys. Rev. Lett. **94**, 046102 (2005).
[17] I. Li, J. Bandara, and M. J. Shultz, Langmuir **20**, 10474 (2004).
[18] Z. Du and N. H. de Leeuw, Surf. Sci. **554**, 193 (2004).
[19] F. Vigné-Maeder and P. Sautet, J. Phys. Chem. B **101**, 8197 (1997).
[20] Y. Ma, A. S. Foster, and R. M. Nieminen, J. Chem. Phys. **122**, 144709 (2005).
[21] T. R. Walsh, M. Wilson, and A. P. Sutton, J. Chem. Phys. **113**, 9191 (2000).
[22] A. Pelmenschikov, H. Strandh, L. G. M. Pettersson, and J. Leszczynski, J. Phys. Chem. B **104**, 5779 (2000).
[23] H.-P. Cheng, R. N. Barnett, and U. Landman, J. Chem. Phys. **116**, 9300 (2002).
[24] M. H. Du, A. Kolchin, and H. P. Cheng, J. Chem. Phys. **119**, 6418 (2003).
[25] A. S. D'Souza and C. G. Pantano, J. Am. Ceram. Soc. **82**, 1289 (1999).
[26] X.-G. Wang, A. Chaka, and M. Scheffler, Phys. Rev. Lett. **84**, 3650 (2000).
[27] N. H. de Leeuw, F. M. Higgins, and S. C. Parker, J. Phys. Chem. B **103**, 1270 (1999).
[28] A. G. Pelmenschikov, G. Morosi, and A. Gamba, J. Phys. Chem. A **101**, 1178 (1997); J. Chem. Phys. **96**, 7422 (1992).
[29] J. Yang, S. Meng, L. F. Xu, and E. G. Wang, Phys. Rev. Lett. **92**, 146102 (2004).
[30] J. Yang, S. Meng, L. F. Xu, and E. G. Wang, Phys. Rev. B **71**, 035413 (2005).
[31] G.-M. Rignanese, A. De Vita, J.-C. Charlier, X. Gonze, and R. Car, Phys. Rev. B **61**, 13250 (2000).
[32] G.-M. Rignanese, J.-C. Charlier, and X. Gonze, Phys. Chem.

Chem. Phys. **6**, 1920 (2004).
[33] V. V. Murashov, J. Phys. Chem. B **109**, 4144 (2005).
[34] P. S. Baram and S. C. Parker, Philos. Mag. B **73**, 49 (1996).
[35] D. L. Doering and T. E. Madey, Surf. Sci. **123**, 305 (1983).
[36] S. Meng, L. F. Xu, E. G. Wang, and S. Gao, Phys. Rev. Lett. **89**, 176104 (2002); S. Meng, E. G. Wang, and S. Gao, Phys. Rev. B **69**, 195404 (2004).
[37] G. Kresse and J. Hafner, Phys. Rev. B **47**, R558 (1993); **49**, 14251 (1994); J. Phys.: Condens. Matter **6**, 8245 (1994); G. Kresse and J. Furthmüller, Comput. Mater. Sci. **6**, 15 (1996); Phys. Rev. B **54**, 11 169 (1996).
[38] J. P. Perdew, J. A. Chevary, S. H. Vosko, K. A. Jackson, M. R. Pederson, D. J. Singh, and C. Fiolhais, Phys. Rev. B **46**, 6671 (1992); Y. Wang and J. P. Perdew, *ibid.* **44**, 13 298 (1991).
[39] D. Vanderbilt, Phys. Rev. B **41**, R7892 (1990).
[40] *An Introduction to the Rock-forming Minerals*, edited by W. A. Deer, R. A. Howie, and J. Zussman (Longman Group, Harlow, 1992).
[41] H. J. Monkhorst and J. D. Pack, Phys. Rev. B **13**, 5188 (1976).
[42] G. Mills and H. Jónsson, Phys. Rev. Lett. **72**, 1124 (1994); G. Mills, H. Jónsson, and G. K. Schenter, Surf. Sci. **324**, 305 (1995).
[43] G. Henkelmann, B. P. Uberuaga, and H. Jónsson, J. Chem. Phys. **113**, 9901 (2000).
[44] B. Fubini, V. Bolis, M. Bailes, and F. S. Stone, Solid State Ionics **32**, 258 (1989).
[45] J. K. Gregory, D. C. Clary, K. Liu, M. G. Brown, and R. J. Saykally, Science **275**, 814 (1997).
[46] G. Held and D. Menzel, Surf. Sci. **316**, 92 (1994).
[47] B. J. Smith, D. J. Swanton, J. A. Pople, H. F. Schaefer III, and L. Radom, J. Chem. Phys. **92**, 1240 (1990).
[48] *The Structure and Properties of Water*, edited by D. Eisenberg and W. Kauzmann (Oxford University Press, New York, 1969).
[49] F. Sim, A. S. Amant, I. Papai, and D. R. Salahub, J. Am. Chem. Soc. **114**, 4391 (1992).